Dynamic Support Interference in High-Alpha Testing

L. E. Ericsson* and J. P. Reding†
Lockheed Missiles & Space Company, Inc., Sunnyvale, California

Dynamic test results of aircraft models at high angles of attack are analyzed with regard to the support interference effects. Single-degree-of-freedom oscillatory tests in pitch or yaw of aircraft configurations are subject to the same type of support interference through the near-wake recirculatory region as is experienced by slender bodies of revolution. Consequently, the measurements can be corrected for support interference using the same methodology. The support interference associated with rotary rigs used in coning experiments is of a different type, being stationary in nature rather than unsteady, with the coning motion inducing a displacement of the vortex wake similar to that caused by side slip in a static test. Performing static tests at varying incidence and side-slip angles with two alternate supports can provide the information needed to correct coning experiments for support interference.

Nomenclature

b = wing span
c = mean aerodynamic chord or d for body alone
d = maximum body diameter
d_B = fuselage base diameter
d_S = sting diameter
d_{SS} = lateral dimension of sting-strut
ℓ = rolling moment, coefficient $C_\ell = \ell/(\rho_\infty U_\infty^2/2)Sb$
L = lift, coefficient $C_L = L/(\rho_\infty U_\infty^2/2)S$
m = pitching moment, coefficient $C_m = m/(\rho_\infty U_\infty^2/2)Sc$
M = freestream Mach number
n = yawing moment, coefficient $C_n = n/(\rho_\infty U_\infty^2/2)Sb$
N = normal force, coefficient $C_N = N/(\rho_\infty U_\infty^2/2)S$
p = pressure, coefficient $C_p = (p-p_\infty)/(\rho_\infty U_\infty^2/2)$
P_N = spin rate of ogive nose tip (Fig. 21)
q = pitch rate about body-fixed pitch axis
q' = angular rate about aerodynamic pitch axis
r_v = radial distance to asymmetric vortex
R = Reynolds number, $R = U_\infty c/\nu_\infty$
S = reference area, effective wing area or $\pi d^2/4$ for body alone
U = wind-fixed axial velocity
$\bar{U}$ = mean convection velocity
V = lateral velocity
x = axial distance from body apex
y = lateral deflection
Y = side force, coefficient $C_Y = Y/(\rho_\infty U_\infty^2/2)S$
α = angle of attack
β = angle of side slip
δ_S = sting deflection angle (Fig. 22)
Δ = increment
ν = kinematic viscosity
ρ = density of air
σ = total flow incidence, $= \sin^{-1}(\sin^2\alpha + \sin^2\beta)^{1/2}$
φ = body-fixed roll angle
φ' = tilt angle between symmetry planes of model and support system
ϕ = coning angle, roll angle of rotary rig around its axis
Ω = dimensionless coning rate, $= \dot{\phi}b/2U_\infty$

Subscripts

A = apex
B = base
c.g. = center of gravity or rotation center
S = sting
SS = sting-strut
V = vortex
∞ = freestream conditions

Superscripts

$(\tilde{\ })$ = generalized parameter, e.g., $\tilde{\varphi}$

Differential Symbols

$$\dot{\phi} = \frac{\partial \phi}{\partial t} \qquad C_{\ell_\sigma} = \frac{\partial C_\ell}{\partial \sigma}$$

$$C_{\ell_q} = \frac{\partial C_\ell}{\partial (cq)/U_\infty} \qquad C_{\ell_{\dot{\sigma}}} = \frac{\partial C_\ell}{\partial (c\dot{\sigma})/U_\infty}$$

$$C_{mq} = \frac{\partial C_m}{\partial (cq)/U_\infty} \qquad C_{m_{\dot{\alpha}}} = \frac{\partial C_m}{\partial (c\dot{\alpha})/U_\infty}$$

Introduction

WHILE the need for dynamic tests at high angles of attack is by now well recognized,[1-3] relatively little attention has been given to the associated support interference problem.[4,5] At the time of the review in Ref. 5, only the static support interference had been investigated. Even now, the present authors know of only two investigations of dynamic support interference at high angles of attack.[6,7]

Available experimental results are analyzed here to explore the possibility of correcting for the high-α dynamic support interference, similar to what has been done at low angles of attack.[8]

Discussion

It is instructive to start by looking at the results obtained by Beyers[7,9] in his systematic investigation of dynamic support interference at high angles of attack on the standard dynamics model (Fig. 1). He found the floor- and side-mounted support systems shown in Figs. 2 and 3, respectively, to give widely different pitching moment results (Fig. 4). The floor-mounted support (Fig. 2) generated an effective flow camber, giving

Presented as Paper 86-0760 at the AIAA 14th Aerodynamic Testing Conference, West Palm Beach, FL, March 5-7, 1986; received April 10, 1986; revision received July 30, 1986.

*Senior Consulting Engineer. Fellow AIAA.
†Staff Engineer. Associate Fellow AIAA.

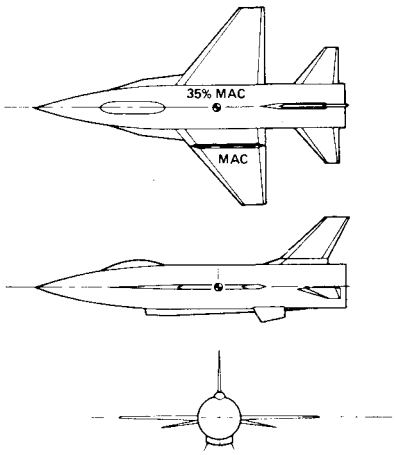

Fig. 1 Standard dynamics model.

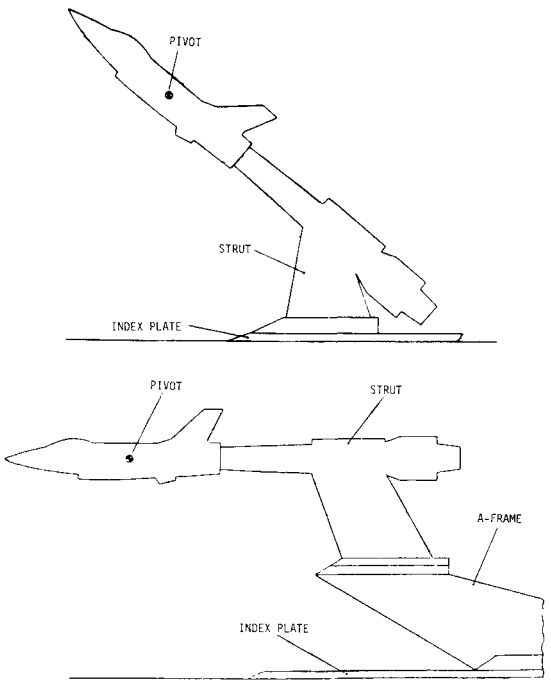

Fig. 2 Floor-mounted support system.[7]

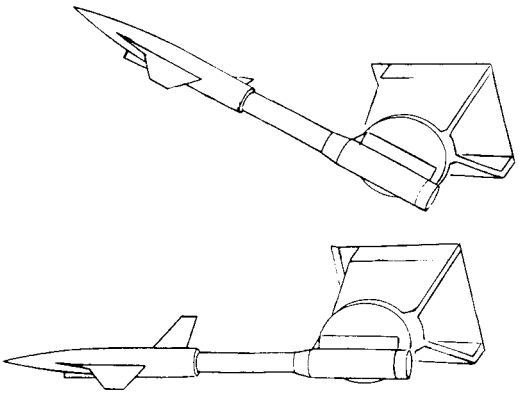

Fig. 3 Sidewall support system.[7]

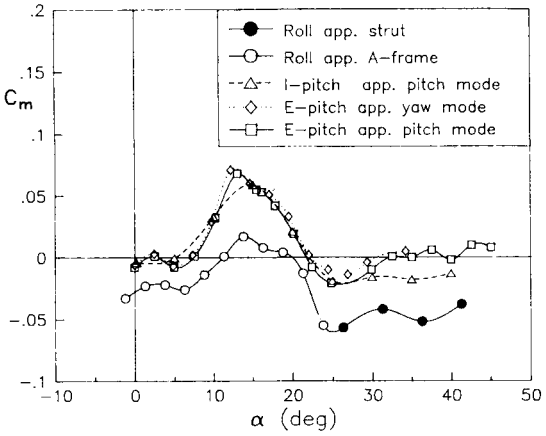

Fig. 4 Comparison of $C_m(\alpha)$ for different supports.[7]

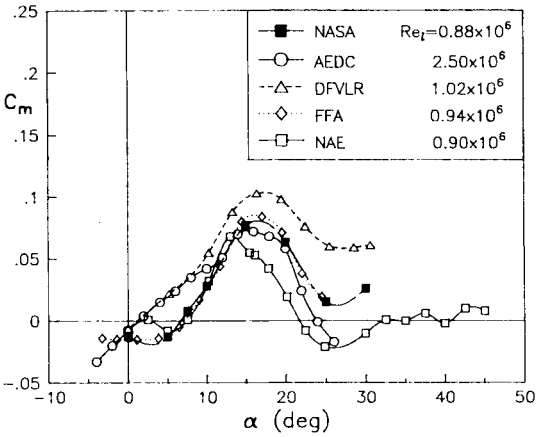

Fig. 5 Interfacility comparison of $C_m(\alpha)$ characteristics.[7]

$C_m < 0$ at $\alpha = 0$. When comparing the results obtained with the side-mounted support[9] (Fig. 3) with those reported by others,[10-13] he found further differences (Fig. 5).

For the floor-mounted support (Fig. 2), Beyers[7] investigated the effect of the tilt angle φ' between the symmetry planes of the model and support system. Whereas the effect on pitch stability measurements was modest, the effect on roll cross-coupling derivatives C_{ℓ_α} and $C_{\ell_{q'}} + C_{\ell_{\dot\alpha}}$ was large at nonzero side slip, $|\beta| = 5$ deg. (See Fig. 6.) The opposition between the support interference effect on static and dynamic derivatives indicates that the interference is associated with a convective flow time lag, similar to what has been found for bodies of revolution.[8]

Before discussing the interaction between free vortices and a downstream support, it is probably worthwhile to note that even in the case of a body of revolution at low angles of attack, the wake is vortical in nature. (See Fig. 7.) As soon as the body crossflow is established, the axisymmetric character of the wake disappears. This explains why even a small-diameter sting can cause a substantial interference effect through the wake deformation at $\alpha \neq 0$ and/or $\beta \neq 0$.[8] The wake vortices become more concentrated at higher angles of attack when they originate on the body itself.

A large effect of the support on lateral characteristics has been reported by Johnson et al.[14] (Fig. 8). The culprit is, in all likelihood, the vortex burst caused by the their curved support. This is the conclusion to be drawn from their repetition of Hummel's classic experiment[15] (Fig. 9), using an arrow wing[14] (Fig. 10). The curved strut design is commonly used in rotary rigs for the performance of coning tests.[16] For a highly swept wing, one can see how the leading-edge vortex can be effected by the curved strut, especially for $\beta \neq 0$.

The vortices generated by a slender nose[17,18] can also interact with a downstream support, especially at very high

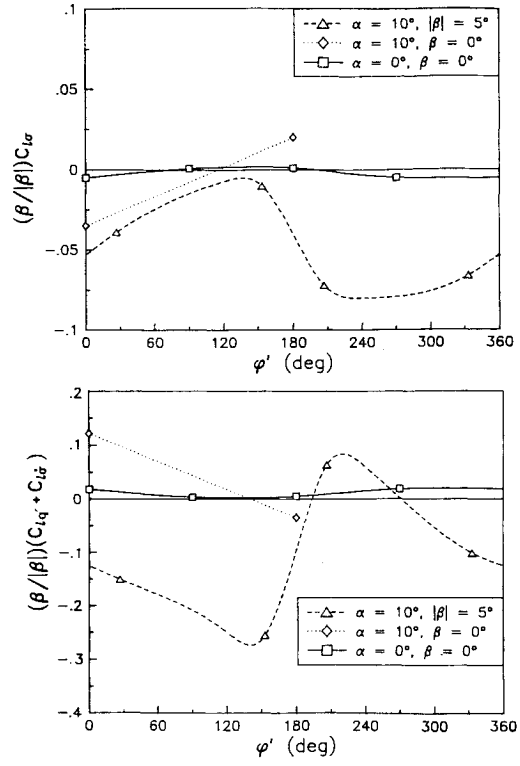

Fig. 6 Effect of model roll angle ϕ' relative to floor-mounted support system on roll-pitch cross-coupling derivatives.[7]

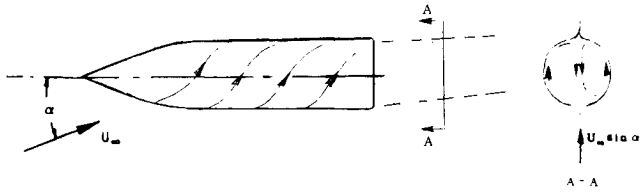

Fig. 7 Vortical wake at $\alpha \neq 0$.

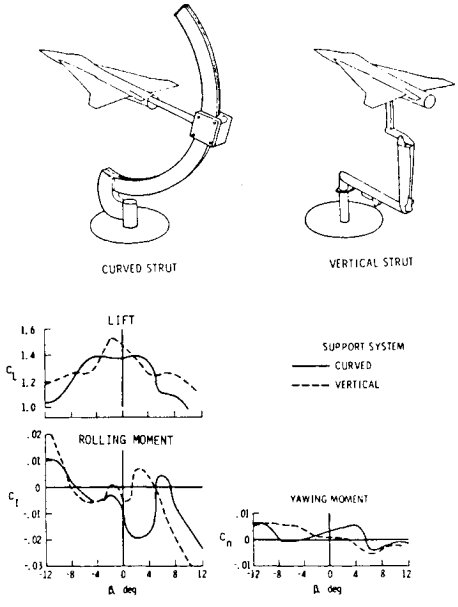

Fig. 8 Effect of model support on lateral characteristics at $\alpha = 35$ deg.[14]

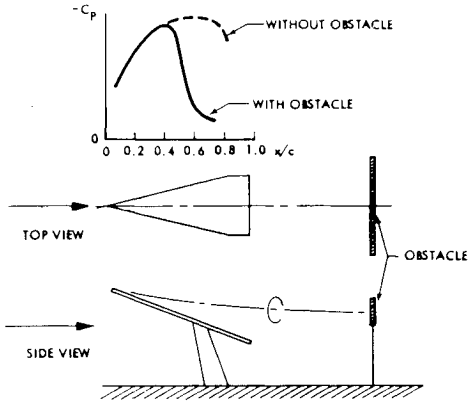

Fig. 9 Vortex burst on a 75-deg delta wing caused by downstream obstacles.[15]

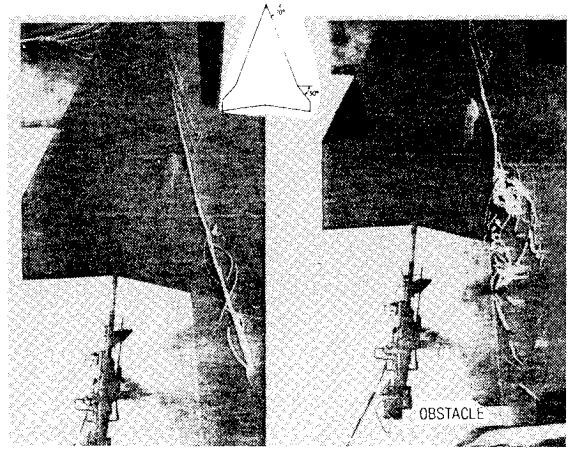

a) No obstacle. b) Obstacle behind model.

Fig. 10 Vortex burst on an arrow wing generated by downstream obstacles.[14]

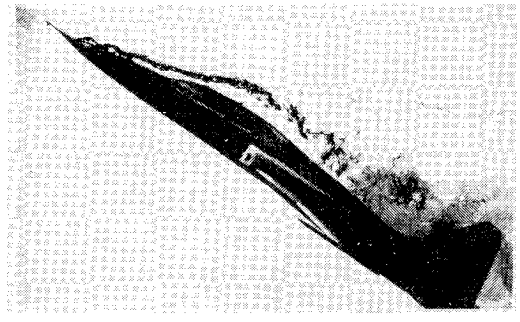

Fig. 11 Asymmetric vortex shedding from the slender nose of an advanced aircraft model at $\alpha = 40$ deg and $\beta = 0$.[19]

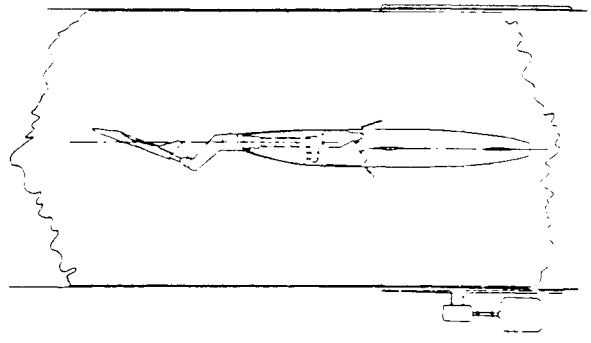

Fig. 12 Typical rotary rig design.[20]

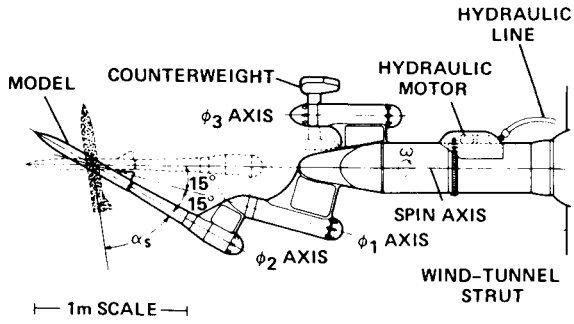

Fig. 13 Rotary rig for coning tests of large aircraft models.[6]

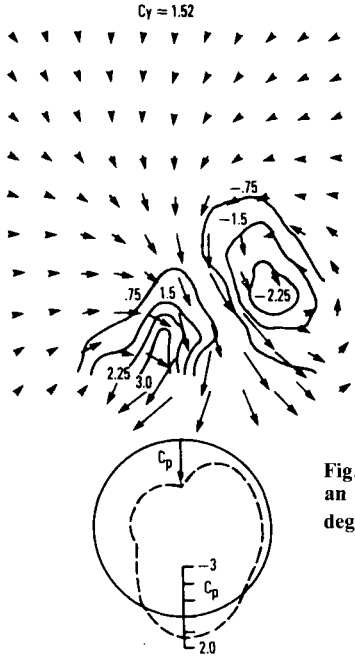

Fig. 14 Flowfield survey above an ogive-cylinder body at $\alpha = 45$ deg.[22]

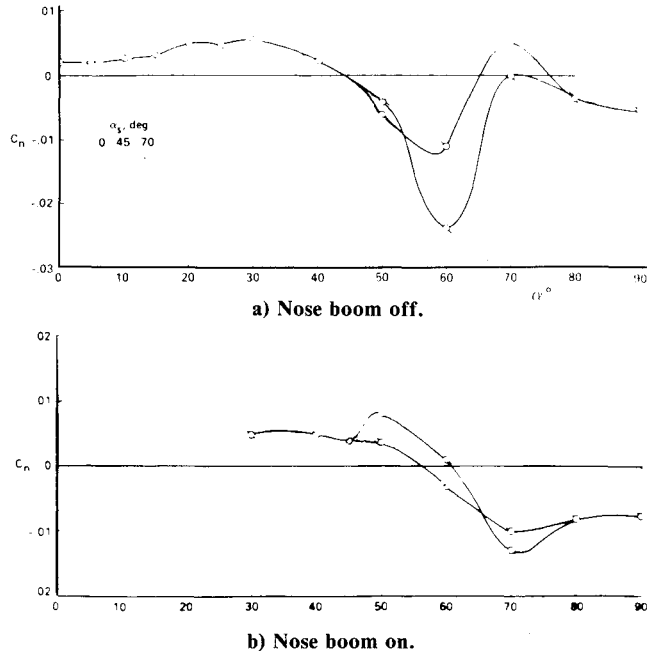

Fig. 15 Effect of α_S on $C_n(\alpha)$ of the F-15 model[6] at $R = 1.5 \times 10^6$.

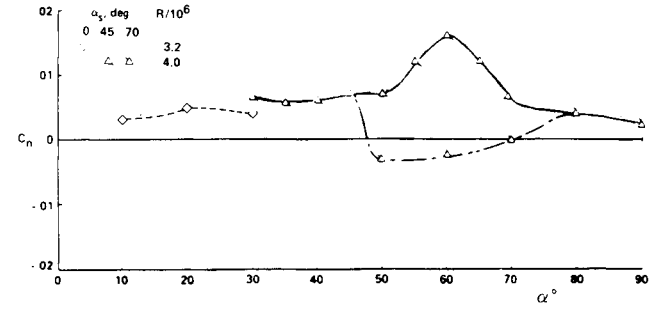

Fig. 16 Effect of α_S and R on $C_n(\alpha)$ of the F-15 model[6] with nose boom on.

angles of attack, when the vortices become asymmetric. In this case, one vortex is left close to the fuselage.[19] (See Fig. 11.) The associated interference effects on the downstream tail surfaces can be severely distorted by a downstream support.

A very common rotary rig design, used by both NASA[13,20] and FFA,[21] is the one shown in Fig. 12. Finally, the rig used by Malcolm[6] for tests of a huge model of the F-15 aircraft is shown in Fig. 13. The sting angle α_S was zero for the aft-mounted model and has the values 45 and 70 deg for the top-mounted model in order to cover the complete angle of attack range $-20 \leq \alpha \leq 90$ deg for small side-slip angles, i.e., $|\beta| \leq 10$ deg. The model was tested with and without a nose boom.

One realizes that the support interference on an asymmetric vortex pair (of the type shown in Fig. 11) will be large for the top-mounted model as the active asymmetric vortex moves inboard close to the center plane[22] (Fig. 14). Its lateral position is determined mainly by the crossflow separation characteristics, as affected by angle of attack, Reynolds number, air turbulence, roughness, moving wall effects, etc. Figure 15 shows that the support interference is similar in nature for $\alpha_S = 45$ and 70 deg. Apparently, asymmetric flow conditions producing a yawing moment at $\beta = 0$ exist even before asymmetric vortex shedding starts (at $\alpha \approx 30$ deg in Fig. 15). The same is true when the Reynolds number is increased above $Re = 1.5 \times 10^6$ (Fig. 16). In this case, the support angle α_S has a large effect; $\alpha_S = 45$ and 70 deg, causing interference effects of the opposite sign in the region of steady asymmetric vortex shedding. Although the region of steady asymmetric vortex shedding can be extended beyond the usual limit ($\alpha \approx 60$ deg, as discussed in Refs. 23 and 24), at $\alpha = 90$ deg the vortex shedding should be of the unsteady type, giving a time average value $C_n = 0$. The nonzero values in Figs. 15 and 16 are likely to have been caused by support interference at $\alpha_S = 45$ and 70 deg of the type found by Dietz and Altstatt[25] (Fig. 17). The loss of normal force is thought to be caused by the splitter-plate-like interaction of the strut with the unsteady Kármán vortex shedding.[26] Similarly, the interaction could prevent the realization of the $C_n = 0$ time average.

In the case of coning test data, the angle α_S affects the C_n characteristics at all angles where asymmetric vortex shedding occurs.[6] The results at $\alpha = 70$ deg (Fig. 18) are apparently of the critical type, similar to the ones found by Fidler for a spinning nose tip[27] (Fig. 19). Thus, the asymmetric vortex geometry is affected strongly by "moving wall" effects,[28,29] causing the steady asymmetric vortex to flip between its two extreme positions, with associated reversals of the yawing moment. (See Fig. 18.)

Correction for Support Interference

It was shown in Ref. 8 how, by performing tests with a deflected sting, one could obtain static test data of the type shown in Fig. 20, from which the sting deflection derivative $C_{m\delta}$ could be obtained. $C_{m\delta}$ could in turn be compared with the stability derivative $C_{m\alpha}$ (Fig. 21), providing the needed clue about the support interference effect on the dynamic stability derivative $C_{mq} + C_{m\dot{\alpha}}$. Obtaining an estimate of the

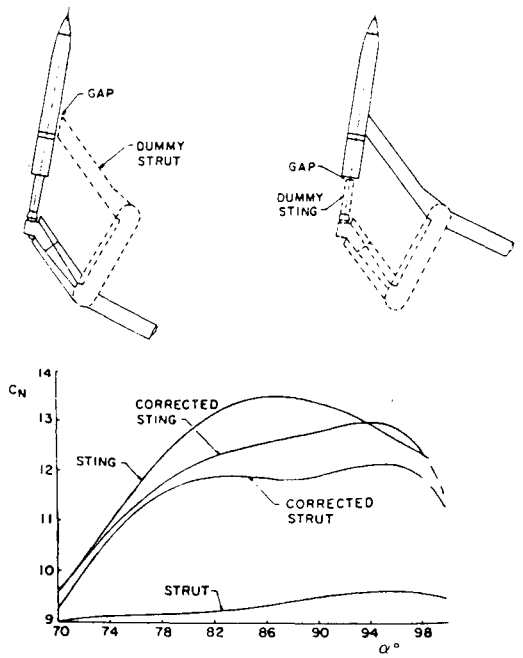

Fig. 17 Effect of leeside support on $C_N(\alpha)$ of an ogive-cylinder model[25] at $M_\infty = 0.6$ and $R = 3 \times 10^6$.

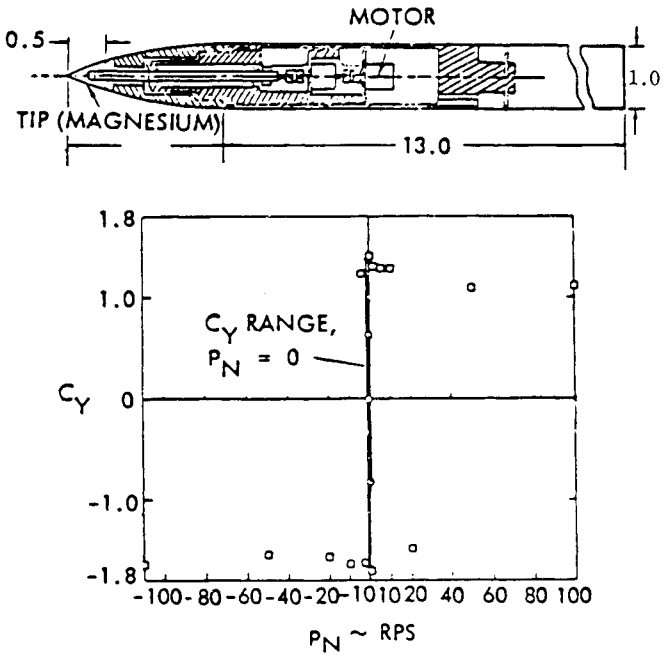

Fig. 19 Effect of spinning nose tip on the side force of an ogive-cylinder at $M_\infty = 0.6$ and $\alpha = 55$ deg.[27]

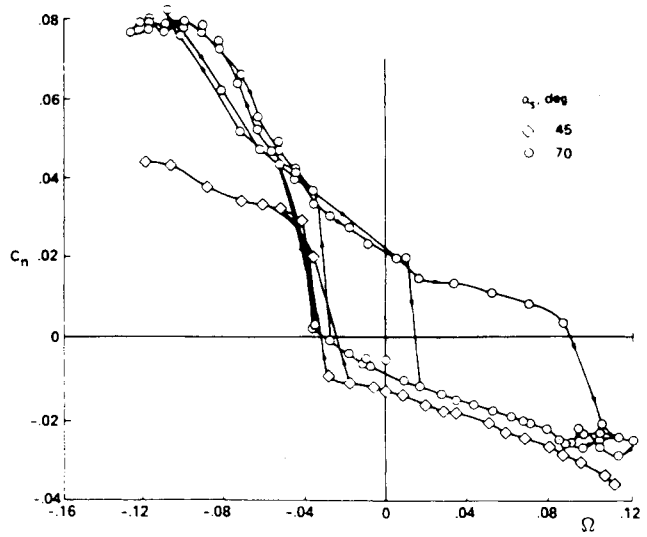

Fig. 18 Effect of α_S on $C_n(\alpha)$ of the F-15 model[6] with nose boom at $R = 1.5 \times 10^6$.

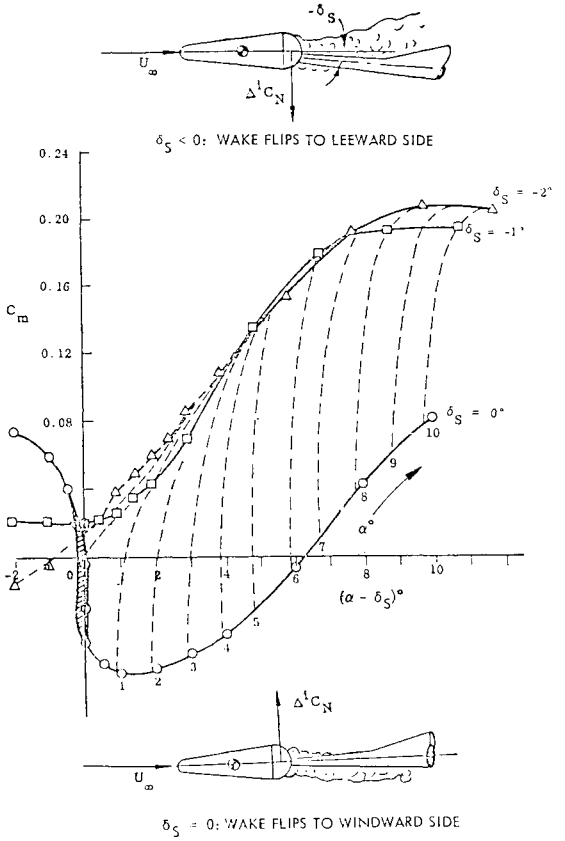

Fig. 20 Pitching moment (α, δ_S) carpet plot[8] at $M_\infty = 0.26$.

convective time lag associated with the support derivative $C_{m\dot{\delta}}$, by assuming that the slender sting had a negligible effect on the recirculation velocities at $\alpha = \beta = 0$, provided the information needed to correct for the support interference[8] (Fig. 22). A similar approach could be used to provided correction for the support interference investigated by Beyers[7,9] (Figs. 1-6). In this case, however, it is very unlikely that the effect of the very bulky support system on the wake recirculation velocities can be neglected. This will complicate the correction procedure, requiring wake velocity measurements in addition to the balance measurements used in the correction procedure described in Ref. 8.

This low α support interference is highly nonlinear, becoming of negligible magnitude as the angle of attack is increased from $\alpha = 0$. Thus, at $\alpha > 10$ deg it is practically nonexistent. As the angle of attack is increased further, however, at some point the support interference on forebody and/or swept wing vortices starts to have a significant influence on the measured aerodynamic characteristics. Although the support geometry is more complex in the case of coning experiments than what it is for one degree-of-freedom oscillations in pitch or yaw, the fluid mechanics of the support interference is simplified considerably. The coning motion is stationary in nature, obviating the need to determine the convective time lag connected with the effect of the downstream support on the upstream model. Thus, one has to determine only the static equivalent to the

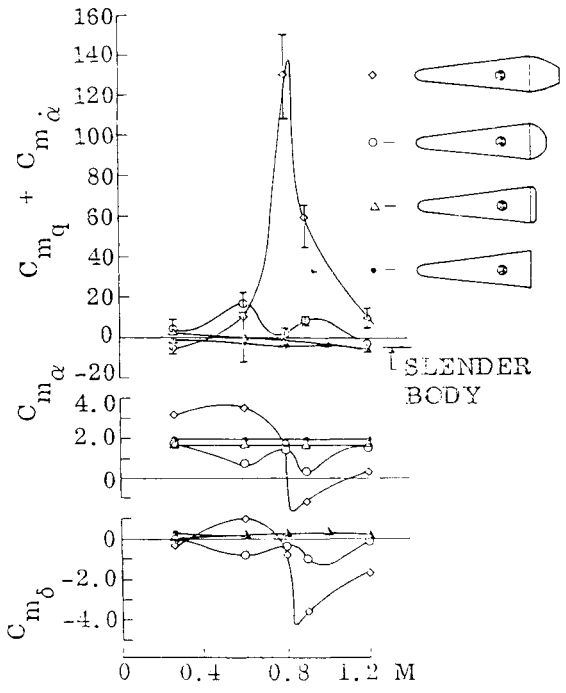

Fig. 21 Correlation of sting-induced moment derivative with static and dynamic stability derivatives.[8]

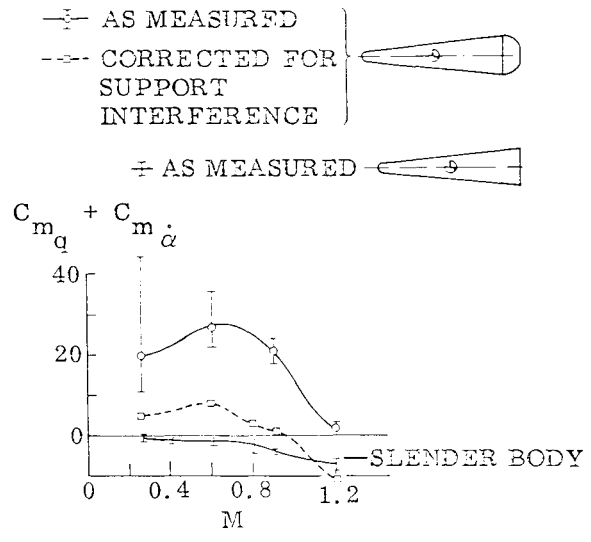

Fig. 22 Damping of hemispherical-based cone corrected for support interference.[8]

coning-induced displacement of the vortical wake or, at very high angles of attack, the free vortices generated by a slender forebody and/or by low-aspect-ratio lifting surfaces.

It is described in Ref. 23 how the various support interference results obtained by Malcolm in his F-15 experiments[6] can be explained when considering how the support amplifies the coning-induced bias of the asymmetric vortex. Another way of inducing such bias is by yawing the model. Even without the occurrence of vortex burst, the support will amplify the β-induced displacement of the vortex. Coning induces a similar displacement of the vortex, a fact well illustrated by Malcolm's results for the F-15 aircraft[6] (Fig. 23). The nose-boom-off data indicate what the results would be if there were no steady asymmetric vortices. The nose boom acts similarly to nose bluntness, extending the range for steady asymmetric vortices beyond the usual limit of $\alpha = 60$ deg.[24]

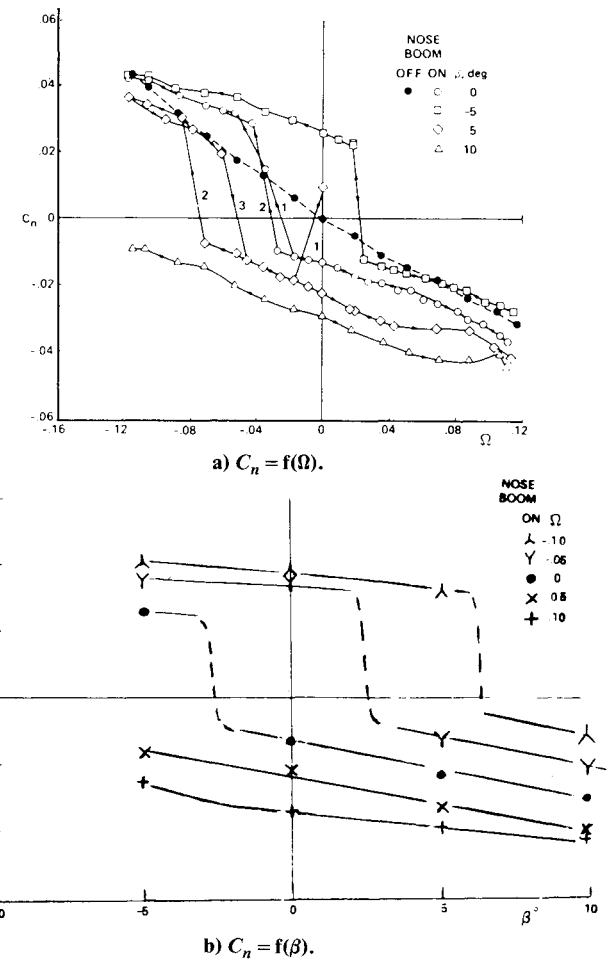

Fig. 23 Effect of side-slip angle β on $C_n(\Omega)$ characteristics of the F-15 model[6] for $\alpha_S = 45$ deg, $\alpha = 70$ deg, and $R = 1.5 \times 10^6$.

Tobak et al.[30] found in their coning test of an ogive cylinder that the symmetric vortex geometry was tilted the angle $\Delta\varphi_A$ along the full length of the body, where $\Delta\varphi_A$ is determined by the coning-induced lateral velocity at apex,

$$\Delta\varphi_A = \tan^{-1}(V_A/U_\infty)$$

$$\frac{V_A}{U_\infty} = \frac{x_{c.g.}}{b}\sin\alpha\,\frac{\dot{\phi}b}{U_\infty} \tag{1}$$

Borrowing the coning sketch from Ref. 13 (Fig. 24), one can see that the vortex will be displaced in the same sense for $\phi > 0$ as for $\beta > 0$. The data points outside of the discontinuities in Fig. 23 give $C_{n\Omega} \approx -0.2$ and $C_{n\beta} \approx -0.1$. With $x_{c.g.} \approx b$ for the F-15 model, Eq. (1) gives $\Delta\varphi_A \approx 1.87\,\Omega$ for $\alpha = 70$ deg. This is in good agreement with the 2/1 ratio between the experimental $C_{n\Omega}$ and $C_{n\beta}$ derivatives. That is, an approximate equivalence between the effects of $\Delta\varphi_A$ and β is indicated, a not totally unexpected result, as the asymmetric vortex pair probably dominates the C_n characteristics at very high angles of attack.

Equation (1) and associated discussion is only valid for the top-mounted model ($\alpha_S = 45$ and 70 deg). In the aft-mounted case ($\alpha_S = 0$), experimental results indicate that there should be no interference effect from a cylindrical sting[31] (Fig. 25). However, there could be a significant interference from the downstream sting-strut (see Fig. 12). After reaching the base of the fuselage, the body vortices will bend off in the freestream direction. In this case, there will be a ϕ-β equivalence, where ϕ is the rotation $\Delta\phi_B = \dot{\phi}\Delta t$ taking place while the vortex travels the distance $(x_{SS} - x_B)$ from the base of the model to the downstream sting-strut. According to Lam-

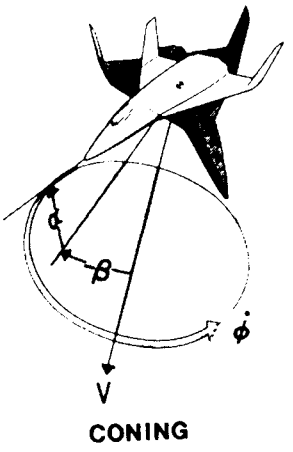

Fig. 24 Definition of variables for coning motion.[13]

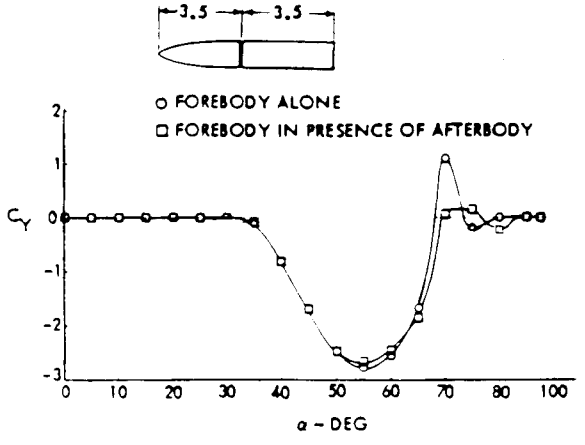

Fig. 25 Effect of cylindrical afterbody on measured side force of a pointed ogive.[32]

bourne et al.'s experiments with delta wing leading-edge vortices,[32] the lateral displacement of the vortex is convected with freestream velocity, $\tilde{U}_V = U_\infty$. Thus,

$$\Delta\phi_B = \frac{x_{SS} - x_B}{d_B} \frac{\dot{\phi} d_B}{U_\infty} \tag{2}$$

The lateral displacement Δy of the vortex relative to the support determines the magnitude of the support interference, with the interference decreasing with increasing Δy until the vortex stays clear of the support.

In the case of $\alpha_S = 45$ or 70 deg, the lateral deflection at the sting (or strut) is $\Delta y_S \approx \tilde{r}_V \tilde{\varphi}$, where $\tilde{\varphi} = \Delta\varphi_A$ for the coning case and $\tilde{\varphi} = \beta$ in the static case. $\tilde{r}_V$ is the vortex location above the fuselage center line. For the coning case, Eq. (1) gives

$$\frac{\Delta y_S}{d_S} = \frac{\tilde{r}_v}{d_S} \frac{x_{\text{c.g.}}}{b} \sin\alpha \frac{\dot{\phi} b}{U_\infty} \tag{3a}$$

Figure 11 indicates that $\tilde{r}_V \approx d_B$ and from Ref. 6 is obtained $x_{\text{c.g.}} \approx b$ and $d_S \approx d_B/2$. For $\Delta y_S > d_S$, one then gets

$$\dot{\phi} b/U_\infty > 0.5 \operatorname{cosec} \alpha \tag{3b}$$

With $\dot{\phi} b/U_\infty = 2\Omega$ and $\alpha = 70$ deg, one obtains the requirement $\Omega > 0.27$, which is outside of the Ω range tested by Malcolm[6] (Fig. 18).

In the $\alpha_S = 0$ case, the lateral deflection at the sting-strut is $\Delta y_{SS} \approx \tilde{r}_{SS} \tilde{\phi}$, where $\tilde{\phi} = -\beta$ in a static test and $\tilde{\phi} = \Delta\phi_B - (\Delta\varphi_A - \Delta\phi_B)$ for the coning case. (Note that $\Delta\phi_B$ is the vortex turning after leaving the body.) $\tilde{r}_{SS}$ is the vortex location above the coning axis at x_{SS} and $(\Delta\varphi_A - \Delta\phi_B)$ is simply $(2 - x_B/x_{\text{c.g.}})\Delta\varphi_A \approx 0$. Thus, Eq. (2) gives

$$\frac{\Delta y_{SS}}{d_{SS}} = \frac{r_{SS}}{b} \frac{x_{SS} - x_B}{d_{SS}} \frac{\dot{\phi} b}{U_\infty} \tag{4a}$$

The values $r_{SS}/b \approx 0.5$ (and $(x_{SS} - x_B)/d_{SS} \approx 10$ appear to be reasonable, giving the following requirement for $\Delta y_{SS} > d_{SS}$:

$$\dot{\phi} b/U_\infty > 0.2 \tag{4b}$$

That is, only $\Omega > 0.1$ is required, a value well within the tested range in Ref. 6.

Thus, if possible one should use the aft-mounted support geometry rather than the top-mounted arrangement illustrated in Fig. 13. The support interference on the vortex will, in general, be less severe in that case. Although the resultant effect on the measured aircraft aerodynamics is very dependent upon tail geometry, one can expect it to be less also. In particular, this would be true for the single-fin geometry. The big advantage is that one should be able to find Ω-β combinations for which the trailing vortex system is well clear of the support, resulting in negligible interference.

Of course, there will always be Ω-β combinations for which the support interference is not negligible. However, it should be possible to correct for the support interference. In addition to performing static and dynamic tests for a range of side-slip angles to obtain an indirect measure of the support interference, one can perform the static test also with an alternate support system, thereby obtaining a direct measurement of the support interference. A candidate for the alternate support is the side-mounted arrangement used by Beyers (Fig. 3).

Conclusions

The following conclusions can be drawn from an analysis of available experimental results.

Oscillatory tests in yaw or pitch of aircraft configurations at low angles of attack are subject to dynamic support interference of the same type as has been experienced for bodies of revolution. Consequently, correction for support interference can be accomplished in a manner similar to that described earlier for slender bodies.

Coning tests are subject to a different type of support interference, being more of a static rather than dynamic nature. Static tests at varying incidence and side-slip angles, employing one additional support system, should provide the information needed to correct for the rotary rig support interference.

References

[1]Orlik-Rückemann, K. J., "Dynamic Stability Testing of Aircraft—Needs vs Capabilities," *Progress in Aerospace Sciences,* Vol. 16, No. 6, Pergamon, New York, 1975, pp. 431-447.

[2]Orlik-Rückemann, K. J., "Aerodynamic Aspects of Aircraft Dynamics at High Angles of Attack," *Journal of Aircraft*, Vol. 20, Sept. 1983, pp. 737-752.

[3]*Dynamic Stability Parameters*, AGARD CP-235, Nov. 1978.

[4]Ericsson, L. E., "A Summary of AGARD FDP Meeting on Dynamic Stability Parameters," AGARD CP-260, Sept. 1978, Paper 2.

[5]Ericsson, L. E. and Reding, J. P., "Review of Support Interference in Dynamic Tests," *AIAA Journal*, Vol. 21, Dec. 1983, pp. 1652-1666.

[6]Malcolm, G. N., "Rotary-Balance Experiments on a Modern Fighter Aircraft Configuration at High Reynolds Numbers," AIAA Paper 85-1829, Aug. 1985.

[7]Beyers, M. E., "Some Recent NAE Experiences of Support Interference in Dynamic Tests," NRC NAE LTR-UA-83, Ottawa, Nov. 1985.

[8]Reding, J. P. and Ericsson, L. E., "Dynamic Support Interference," *Journal of Spacecraft and Rockets,* Vol. 9, July 1972, pp. 547-553.

[9]Beyers, M. E., "SDM Pitch- and Yaw-Axis Stability Derivatives," AIAA Paper 85-1827, Aug. 1985.

[10]Coulter, S. M. and Marquart, E. J., "Cross and Cross-Coupling Derivative Measurements on the Standard Dynamics Model at AEDC," AIAA Paper 82-0596, March 1982.

[11]Torngren, L., "Dynamic Pitch and Yaw Derivatives for the Standard Dynamics Model," FFA TN 1985-5, 1985.

[12]Schmidt, E., "Standard Dynamics Model Experiments with the DFVLR/DVA Transonic Derivative Balance," AGARD CP-386, Nov. 1985, Paper 21.

[13]Jermey, C. and Schiff, L. B., "Wind Tunnel Investigation of the Aerodynamic Characteristics of the Standard Dynamics Model in Coning Motion at Mach 0.6," AIAA Paper 85-1828, Aug. 1985.

[14]Johnson, J. L. Jr., Grafton, S. B., and Yip, L. P. "Exploratory Investigation of Vortex Bursting on the High-Angle-of-Attack Lateral Directional Stability Characteristics of Highly Swept Wings," AIAA Paper 80-0463, March 1980.

[15]Hummel, D. "Untersuchungen über das Aufplatzen der Wirbel an schlanken Delta Flügeln," *Zeitschrift für Flugwissenschaften*, Vol. 13, No. 5, 1965, pp. 158–168.

[16]O'Leary, C. and Rowthorn, E.N., "New Rotary Rig at RAE and Experiments on HIRM," AGARD CP-386, Nov. 1985, Paper 19.

[17]Ericsson, L. E. and Reding, J. P., "Review of Vortex-Induced Asymmetric Loads—Part I," *Zeitschrift für Flugwissenschaften Weltraumforschung*, Vol. 5, No. 3, 1981, pp. 162–174.

[18]Ericsson, L. E. and Reding, J. P., "Review of Vortex-Induced Asymmetric Loads—Part II," *Zeitschrift für Flugwissenschaften Weltraumforschung,* Vol. 5, No. 6, 1981, pp. 349–366.

[19]Skow, A. M., Moore, W. A., and Lorincz, D. J., "Forebody Vortex Blowing—A Novel Control Concept to Enhance Departure/Spin Recovery Characteristics of Fighter and Trainer Aircraft," AGARD CP-262, Sept. 1979, Paper 24.

[20]Henderson, W. P., Phillips, W. P., and Gainer, T. G., "Rolling Stability Derivatives of a Variable Sweep Fighter Model at Subsonic and Transonic Speeds," NASA TND-3845, 1967.

[21]Jansson, T. and Torngren, L., "New Dynamic Testing Techniques and Related Results at FFA," AGARD CP-386, Nov. 1985, Paper 20.

[22]Wardlaw, A. B. J. and Yanta, W. J., "Multistable Vortex Patterns on Slender, Circular Bodies at High Incidence," *AIAA Journal,* Vol. 20, April 1982, pp. 509–515.

[23]Ericsson, L. E., "Reflections Regarding Recent Rotary Rig Results," AIAA Paper 86-0123, Jan. 1986.

[24]Ericsson, L. E. and Reding, J. P., "Alleviation of Vortex-Induced Asymmetric Loads," *Journal of Spacecraft and Rockets,* Vol. 17, Nov.–Dec. 1980, pp. 548–553.

[25]Dietz, W. E. and Altstatt, M. C., "Experimental Investigation of Support Interference on an Ogive-Cylinder at High Incidence," *Journal of Spacecraft and Rockets,* Vol. 16, Jan.–Feb. 1979, pp. 67–68 (see also AIAA Paper 78-165, Jan. 1978).

[26]Nelson, R. C. and Mouch, T. N., "Cylinder-Splitter-Plate Data Illustrating High-α Support Interference," *Journal of Spacecraft and Rockets,* Vol. 16, March–April 1979, pp. 126–128.

[27]Fidler, J. E., "Active Control of Asymmetric Vortex Effects," *Journal of Aircraft,* Vol. 18, April 1981, pp. 267–272.

[28]Ericsson, L. E., "Karman Vortex Shedding and the Effect of Body Motion," *AIAA Journal,* Vol. 18, Aug. 1980, pp. 935–944.

[29]Ericsson, L. E. and Reding, J. P., "Dynamics of Forebody Flow Separation and Associated Vortices," *Journal of Aircraft,* Vol. 22, April 1985, pp. 329–335.

[30]Tobak, M., Schiff, L. B., and Peterson, V. L., "Aerodynamics of Bodies of Revolution in Coning Motion," *AIAA Journal*, Vol. 7, Jan. 1969, pp. 95–99.

[31]Keener, E. R., Chapman, G. T., and Kruse, R. L., "Effects of Mach Number and Afterbody Length on Onset of Asymmetric Forces on Bodies at Zero Sideslip and High Angles of Attack," AIAA Paper 76-66, Jan. 1976.

[32]Lambourne, N. C., Bryer, D. W., and Maybrey, J. F. N., "The Behavior of the Leading-Edge Vortices Over a Delta Wing Following a Sudden Change of Incidence," British Aeronautical Research Council, R&M 3645, March 1969.